

# UV-illuminated dielectrophoresis by two-dimensional electron gas (2DEG) in AlGa<sub>N</sub>/Ga<sub>N</sub> heterojunction

Junxue Fu<sup>1\*,1</sup>, Yuan Luo<sup>2</sup>, Levent Yobas<sup>2</sup>, and Kevin J. Chen<sup>2</sup>

<sup>1</sup>Department of Physics, Hong Kong Baptist University, Kowloon Tong, Hong Kong

<sup>2</sup>Department of Electronic and Computer Engineering, Hong Kong University of Science and Technology, Clear Water Bay, Hong Kong

Received 16 January 2012, revised 5 July 2012, accepted 13 July 2012

Published online 29 August 2012

**Keywords** dielectrophoresis, heterojunctions, two-dimensional electron gas

\* Corresponding author: e-mail phyjxfu@hkbu.edu.hk, Phone: (852) 3411 5157, Fax: (852) 3411 5813

<sup>†</sup> These two authors contributed equally to this work.

Dielectrophoresis (DEP) induced by activating a patterned two-dimensional electron gas (2DEG) at the interface of compound semiconductor AlGa<sub>N</sub>/Ga<sub>N</sub> heterojunction has been demonstrated for the first time in our previous work. Briefly, with a peak voltage of  $\pm 10$  V and a frequency from 100 kHz to 1 MHz, characteristics of both positive and negative DEP have been observed successfully manipulating 2  $\mu$ m polystyrene microspheres in a drop of deionized (DI) water (pH  $\sim 7$  and conductivity  $1 \times 10^{-4}$  S m<sup>-1</sup>) over castellated 2DEG electrodes

separated by critical dimensions 50 and 150  $\mu$ m. This study reports a peculiar observation encountered when performing the DEP experiments under ultraviolet (UV) radiation: The microspheres have been repelled from the 2DEG electrodes yet remained on the surface during pDEP and then levitated upon switching to nDEP. This behavior is not observed in DEP with conventional microelectrodes and explained here by the UV-induced electron–hole generation and the subsequent charge redistribution in the AlGa<sub>N</sub>/Ga<sub>N</sub> heterostructure.

© 2012 WILEY-VCH Verlag GmbH & Co. KGaA, Weinheim

**1 Introduction** Dielectrophoresis (DEP), a popular technique widely utilized to separate and enrich cells and microparticles in suspension, is identified with dielectric particles experiencing a net motive force in the presence of spatially non-uniform electric field. The DEP force acts in the direction of the field gradient, attracting particles to the field maxima if they are more polarized than the suspending medium or else repelling them from the field maxima. The former is referred to as the positive DEP (pDEP) whereas the latter the negative DEP (nDEP) [1]. The DEP technique has been widely used in numerous applications including isolation of colloidal or virus particles [2, 3], detection of DNA [4] and microorganisms [5] and the enrichment of DNA, bacteria, and analytes [6].

The DEP-based technologies are diverse and yet not without their specific drawbacks. DEP through thin-film metal microelectrodes often introduces water hydrolysis and subsequent generation of gas bubbles around the microelectrodes [7, 8]. Thin-film microelectrodes may lose functionality due to fouling as well [9]. Insulator-based or electrodeless DEP alleviates some of these drawbacks by

replacing microelectrodes with a set of insulating microstructures which perturb field lines between a pair of external electrodes supplied with DC and/or AC voltage [10–16]. Yet the technique requires high voltages which often induces electrophoresis and excessive joule heating in a biologically relevant medium [17, 18]. Contactless DEP utilizes a body of electrolyte isolated by a thin insulating partition as a “liquid” electrode [19, 20]. The shape and the separation of the “liquid” electrodes are determined by the layout of the microchannels. Although the partition can be made microscopically small, it requires fairly high-alternating current (AC) excitation to couple the field into the particle medium.

A new kind of integrated microelectrodes for inducing DEP based on a high-density two-dimensional electron gas (2DEG) has been introduced in our previous work [21]. The 2DEG forms in the chemically inert and biologically compatible AlGa<sub>N</sub>/Ga<sub>N</sub> heterojunction interface owing to spontaneous and piezoelectric polarization effects (Fig. 1a) [22]. The spontaneous (intrinsic) polarization in the AlGa<sub>N</sub> film arises from a polar hexagonal structure of the Ga<sub>N</sub> crystal along the growth direction. The growth technique

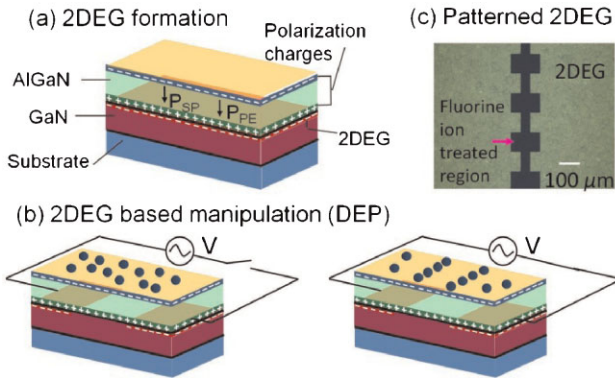


**Figure 1** (online color at: www.pss-a.com) (a) 2DEG formation at the heterojunction interface between AlGaIn film and GaN crystal; (b) 2DEG channel patterned as electrodes inducing DEP for the manipulation of microparticles. (c) Image of AlGaIn/GaN surface with a castellated 2DEG pattern visible under UV illumination.

adopted here, metal oxide chemical vapor deposition (MOCVD) yields a spontaneous polarization ( $P_{SP}$ ) that is always opposite to the growth direction (away from the surface). Moreover, the thin layer of AlGaIn develops a tensile stress to match the lattice constant of the GaN crystal. The tensile stress leads to a piezoelectric polarization ( $P_{PE}$ ) that aligns with the spontaneous polarization. Superposition of the two polarizations aligned in the same direction yields a high-density fixed negative charge at the AlGaIn surface and a high-density fixed positive charge at the heterostructure interface. The former is compensated by donor-like surface states whereas the latter induces a high-density 2DEG at the heterostructure interface [23]. Such high-electron density ( $\sim 10^{13} \text{ cm}^{-2}$ ) along with high mobility ( $\sim 1500 \text{ cm}^2 \text{ V}^{-1} \text{ s}^{-1}$ ) yields a highly conductive channel (2DEG) with a resistivity as low as 200–300  $\Omega \text{ cm}$ . When properly patterned with ionized fluorine as prescribed in our earlier studies, the 2DEG channel can be configured into microelectrodes that can be activated for DEP manipulation as schematically described in Fig. 1b. Unlike the microelectrodes defined by a thin-film metal, the 2DEG electrodes maintain no direct contact with the analyte, and thus offer the merits of both the insulator-based DEP and the contactless DEP.

Figure 1c is an image of the castellated patterned 2DEG electrodes, which become visible under UV illumination (wavelength: 320–380 nm) as the light absorbed gets re-emitted via band edge emission in the regions not treated with ionized fluorine. In this letter, a peculiar observation will be reported when performing the DEP experiments under ultraviolet (UV) radiation, which seems to offer extra control parameter in 2DEG based DEP.

**2 Theory** The DEP force arises from the induced polarization in a non-uniform electric field and can be expressed for a spherical particle in time-average form as [1]

$$F_{\text{DEP}} = 2\pi R^3 \epsilon_m \text{Re}\{K(\omega)\} \nabla(\mathbf{E}_{\text{rms}} \cdot \mathbf{E}_{\text{rms}}), \quad (1)$$

where  $R$  is the radius of the particle,  $\epsilon_m$  the permittivity of the suspending medium,  $E_{\text{rms}}$  the electric field (root mean square) with radial frequency  $\omega$  and  $K(\omega)$  the Clausius–Mossotti (CM) factor. The CM factor depends on the complex permittivity of the particle  $\epsilon_p^*$  and of the suspending medium  $\epsilon_m^*$ :

$$K(\omega) = \frac{\epsilon_p^* - \epsilon_m^*}{\epsilon_p^* + 2\epsilon_m^*}, \quad (2)$$

whereas complex permittivity, for any material, can be given by

$$\epsilon^* = \epsilon + \frac{\sigma}{j\omega}, \quad (3)$$

where  $\epsilon$  and  $\sigma$  are the real permittivity and conductivity of the material ( $j = \sqrt{-1}$ ). In (1), the sign or the direction of the DEP force is determined by the real part of the CM factor, which assumes a value between  $-0.5$  and  $+1$  depending on the polarizability of the spherical particle and of the suspending medium. If the particle is more polarized than the medium,  $\text{Re}\{K(\omega)\}$  becomes positive and the particle is pulled up the field gradient under positive DEP (pDEP). If the particle is less polarized than the medium,  $\text{Re}\{K(\omega)\}$  becomes negative and the particle is repelled down the field gradient under negative DEP (nDEP). As the CM factor depends on  $\omega$ , the direction of the induced force can be conveniently switched by changing the frequency of the applied field rather than changing the suspending medium.

**3 Materials and methods** The 2DEG based DEP device fabrication has been described elsewhere [21]. In brief, we used a commercial  $\text{Al}_{0.26}\text{Ga}_{0.74}\text{N}/\text{GaN}$  including a 1.8  $\mu\text{m}$  GaN buffer, a 17.5 nm undoped AlGaIn layer, and a 2 nm undoped GaN cap. The DEP electrodes were patterned by selectively subjecting the 2DEG to fluorine plasma at an RF power of 300 W for 100 s in an RIE system (Surface Technology Systems) [24, 25]. Due to strong electronegativity of fluoride ions ( $\text{F}^-$ ) and their high energy, the 2DEG was effectively quenched in areas exposed to the plasma. Reproducibility of the 2DEG patterns across various batches was confirmed through leakage currents consistently measured as  $10^{-12} \text{ A}$  (at 1 V) between the 2DEG electrodes apart by 50  $\mu\text{m}$ . The electrodes separated by 5  $\mu\text{m}$  gap sustained a break-down voltage of 172 V (at a current of 0.1  $\text{mA mm}^{-1}$ ).

As shown in Fig. 2a, the sample chips, each containing 12 device units, were individually secured in a package (CCF01434, SPECTRUM) by epoxy. Electrical contacts were made via wire bonding. The packaged chips received a conformal deposition of 1- $\mu\text{m}$ -thick parylene C as a sealing material. For the DEP experiments carboxylated fluorescent polystyrene microspheres (Bangs Laboratories, Inc. diameter 2 or 10  $\mu\text{m}$ ) suspended in DI water (pH  $\sim 7$  and  $1 \times 10^{-4} \text{ S m}^{-1}$ ) were manually pipetted into the package and a cover slip was placed to minimize evaporation (Fig. 2b).

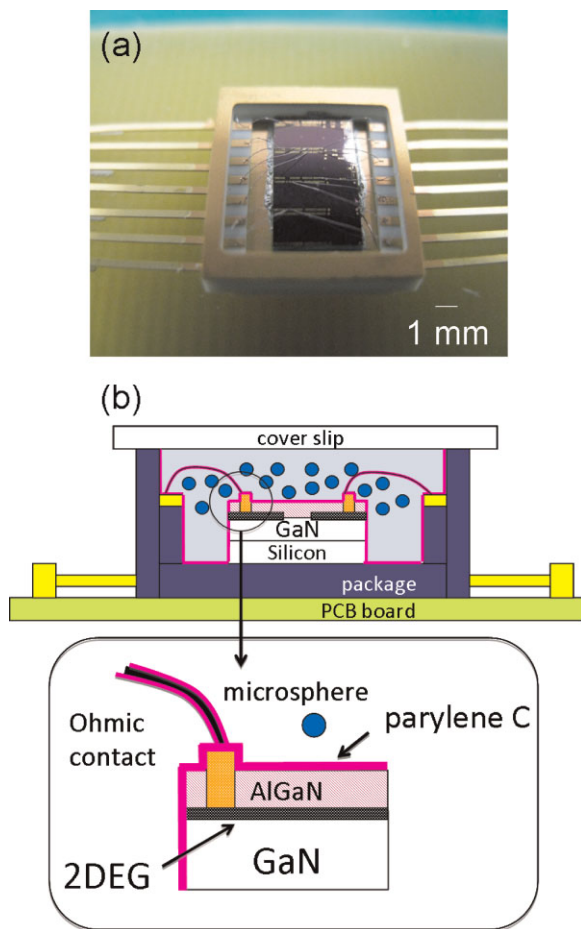


**Figure 2** (online color at: www.pss-a.com) (a) Photograph of a packaged GaN/AlGaN chip with patterned 2DEG microelectrodes and (b) a cross-sectional schematic description of the experimental setup for the DEP manipulation of microspheres suspended over patterned 2DEG.

The microspheres were negatively charged due to the presence of residual sulfate groups leftover from their synthesis (anionic surfactants and initiators) as well as due to the carboxyl surface groups negatively charged in a DI water at  $\text{pH} \sim 7$ . The 2DEG electrodes were driven by an alternating current with the frequency ranging from 10 kHz to 10 MHz (Agilent HP 8114A) and the peak voltage up to  $\pm 10$  V.

**4 Results and discussion** The gradient of the squared electric field of the castellated electrodes was simulated by COMSOL Multiphysics Software 3.5. As depicted by the gradient of the squared electric field intensity in Fig. 3a, the intensity is the strongest at the edges of the electrodes along the narrow segments, relatively less along the wide segments, and reaches minimum at the center of each wide segment. Since the direction of the DEP force follows the field gradient, the pDEP is expected to occur along the electrode edges (within both the narrow and wide

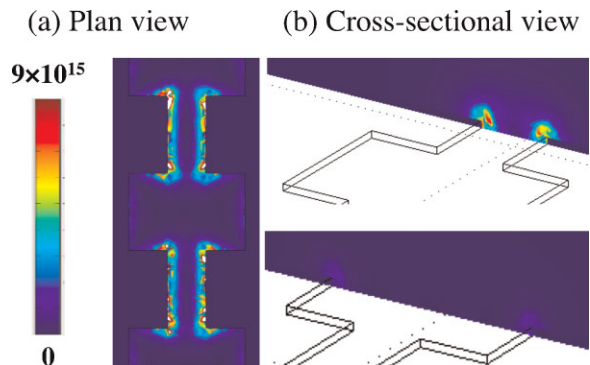


**Figure 3** (online color at: www.pss-a.com) Gradient of the squared electric field intensity ( $\text{V}^2 \text{m}^{-3}$ ) simulated across the gap between the castellated 2DEG electrodes, (a) top view and (b) cross-sectional view along the narrow gap (above) and the wide gap (below) for the excitation  $\pm 10$  V peak.

segments) and the nDEP at the center of the wide segments. The gradient of the squared electric field in vertical direction is also indicated in Fig. 3b and accordingly during nDEP there should be an upward force levitating microspheres.

Our previous work [21] demonstrated DEP experiments carried out under the white light illumination and the findings are briefly summarized here. During the excitation with a voltage of 100 kHz and  $\pm 10$  V peak, pDEP was observed with the castellated patterned 2DEG electrodes shown in Fig. 1c. The microspheres were concentrated at the edges of the gap between the electrodes within both the narrow and wide segments (inset in Fig. 4a). Upon switching to 1 MHz while maintaining the magnitude, nDEP was encountered. The microspheres were immediately migrated toward the center of the wide segments where the field gradient was the weakest (inset in Fig. 4b). The crossover frequency has been experimentally determined as 300–400 kHz. The chip was occasionally exposed to UV illumination only briefly to image the distribution of microspheres with respect to the 2DEG electrodes. The above observations under the white light illumination are consistent with the simulated results and concur the earlier accounts of DEP using surface metal microelectrodes. Though there is a force pushing microspheres upwards during nDEP ( $< 10^{-14}$  N) [26], they still stayed on the surface partially due to the gravity ( $\sim 10^{-15}$  N).

The present work reports on a more interesting behavior of microspheres encountered when the above DEP experiments repeated here under the UV illumination. Figure 4 shows time-lapsed images of the experiment for both pDEP and nDEP. Initially, the microspheres were evenly spread ( $t = 0$  s). During pDEP (100 kHz and  $\pm 10$  V), the microspheres formed chains along a straight line distanced from both electrodes ( $t = 36$  s). Within seconds, the microspheres began to migrate along the line toward the narrow gaps ( $t = 54$  s). This is in contrast with pDEP observed under visible light where the microspheres in both the narrow and wide gaps remained rather attracted toward both electrodes (the inset) [21]. Upon switching to nDEP (1 MHz and

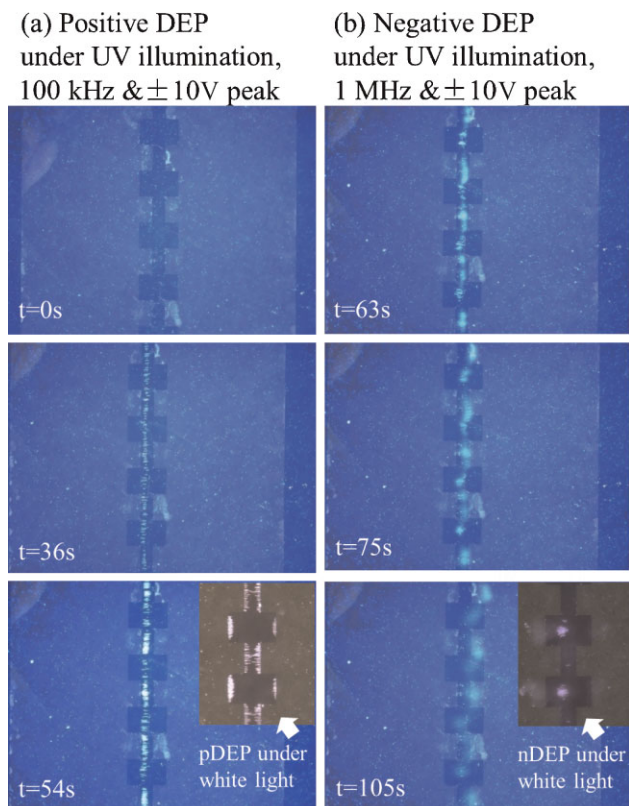


**Figure 4** (online color at: [www.pss-a.com](http://www.pss-a.com)) Time-lapse images showing distributions of 2  $\mu\text{m}$ -diameter polystyrene microspheres in DI water on the castellated 2DEG electrodes as a result of (a) pDEP (100 kHz,  $\pm 10$  V peak) and (b) nDEP (1 MHz,  $\pm 10$  V peak) all performed under UV illumination. Insets: pDEP (100 kHz,  $\pm 10$  V peak) and nDEP (1 MHz,  $\pm 10$  V peak) under white light illumination.

$\pm 10$  V), the microspheres began to levitate appearing out of focus initially within the narrow gaps ( $t = 63$  s), followed by those within the wide gaps ( $t = 75$  s). These microspheres continued to levitate with the UV illumination ( $t = 105$  s). This behavior differs from the observation of nDEP in the absence of UV illumination (the inset), which seems to offer extra control parameter in DEP.

Further experimental investigation has been carried out here using larger polystyrene microspheres 10  $\mu\text{m}$  in diameter. Their crossover frequency ( $< 5$  kHz) was found to be much lower than that of 2  $\mu\text{m}$  microspheres possibly due to distinct surface conductance [27, 28]. To avoid low-frequency electrokinetic effects, the subsequent experiments were performed at 100 kHz and mainly focused on nDEP where the effect of UV illumination on the particle levitation could be investigated. Figure 5a shows time-lapsed images of an experiment performed under UV illumination. The microspheres were randomly distributed over the 2DEG electrodes prior to the application of the excitation ( $t = 0$  s). With the excitation voltage at  $\pm 5$  V peak, the microspheres were repelled from the 2DEG electrodes and confined to the center of the wide segments of the gap where the field was

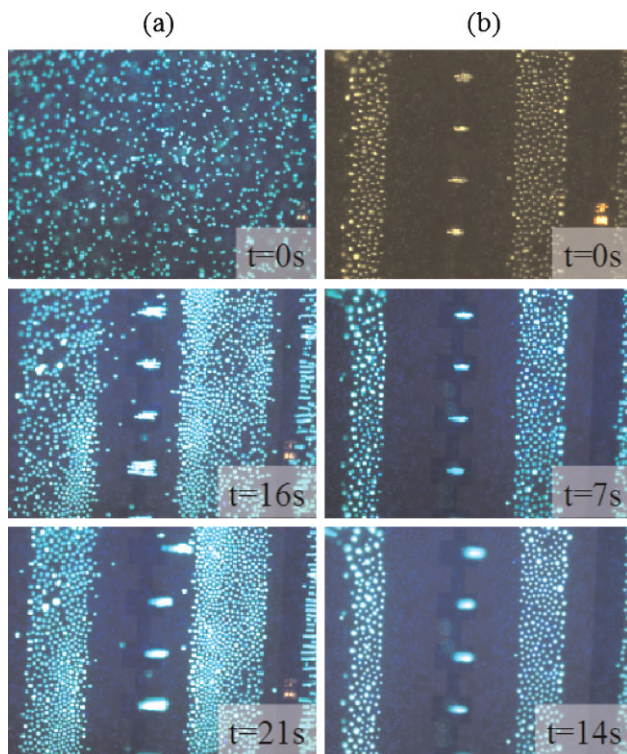


**Figure 5** (online color at: [www.pss-a.com](http://www.pss-a.com)) Time-lapse images showing distributions of 10  $\mu\text{m}$ -diameter polystyrene microspheres in DI water on the castellated 2DEG electrodes as a result of nDEP at 100 kHz: (a) performed under the UV illumination; shown before applying any voltage (0 s); at  $\pm 5$  V peak (16 s); and the levitation begins at  $\pm 7.5$  V peak (21 s); (b) at  $\pm 5$  V peak under the white light illumination (0 s) and immediately after switching to the UV illumination (7 s) and shortly after which the levitation begins (14 s).

minimum ( $t = 16$  s). However, the net force on the microspheres was not sufficient to levitate them. The levitation began when the excitation voltage was increased to  $\pm 7.5$  V peak ( $t = 21$  s). Another experiment was performed on the device after randomly redistributing the microspheres over the electrodes. As shown in Fig. 5b, the excitation at  $\pm 5$  V peak was sufficient to form the nDEP pattern under white light illumination but not adequate to levitate the microspheres ( $t = 0$  s). While keeping the excitation magnitude at  $\pm 5$  V peak, the illumination was switched to UV ( $t = 7$  s) and then shortly afterwards the levitation was noticed ( $t = 14$  s). Interestingly, this excitation magnitude did not lead to levitation in the previous experiment with the UV illumination constantly on. Clearly the UV illumination has a profound effect on the larger microspheres in comparison.

The peculiar behavior of the 2DEG-based DEP under the UV illumination is most likely related to the generation of electron-hole pairs in GaN (with a 3.4 eV bandgap corresponding to a wavelength of 349 nm) and subsequent charge redistribution in the AlGaN/GaN heterostructure. This point is further elaborated by the band diagrams and free body diagrams in Fig. 6. As described by the band diagram in

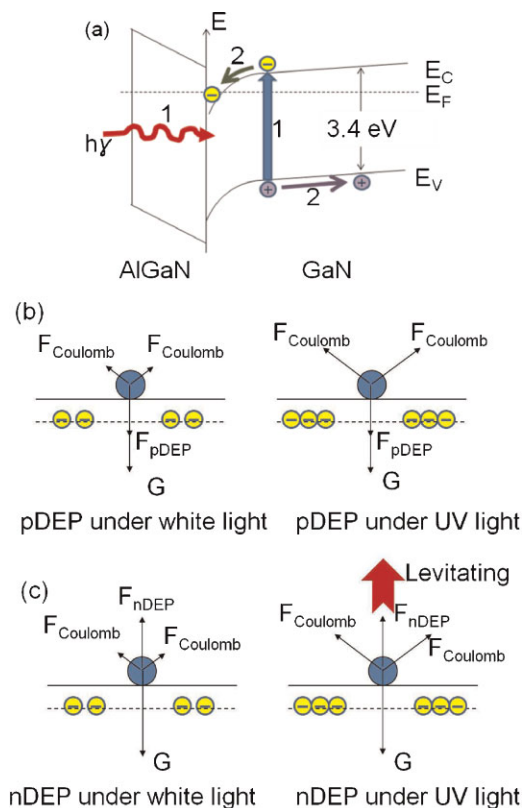


**Figure 6** (online color at: [www.pss-a.com](http://www.pss-a.com)) (a) The energy band diagram of AlGaIn/GaN heterostructure describing the UV-induced generation of electron–hole pairs (Process 1) and the redistribution of electrons and holes (Process 2). Schematic description of the forces exerted on a single microsphere during DEP manipulation with the 2DEG under white light or UV illumination: (b) positive DEP and (c) negative DEP. ( $E_C$ , conduction band energy;  $E_V$ , valence band energy;  $E_F$ , Fermi energy; and G, gravity).

Fig. 6a, electron–hole pairs are generated under UV illumination (Process 1): the electrons in the valence band absorb the energy of UV photons and jump to the conduction band, leaving holes in the valence band. The electric field at the AlGaIn/GaN heterostructure points toward the hetero-interface, resulting in further electron accumulation near the surface while the holes tend to move away from the surface toward the GaN bulk (Process 2). These electrons charge up the electrodes and exert stronger repulsive Coulomb force on the negatively charged microspheres. The repulsive force, although it becomes sufficient to confine the microspheres to a straight line, falls short of levitating them due to stronger pDEP acting in the opposing direction (Fig. 6b). In further response to pDEP, the microspheres migrate toward the narrow gaps where the field intensity is high. Upon switching the polarity of DEP, the microspheres overcome the gravity and levitate under the synergetic action of the repulsive Coulomb and nDEP forces (Fig. 6c).

One may notice that the microspheres after being levitated moved toward the 2DEG on the right side ( $t = 105, 21, \text{ and } 14 \text{ s}$  in Figs. 4b and 5a,b, respectively).

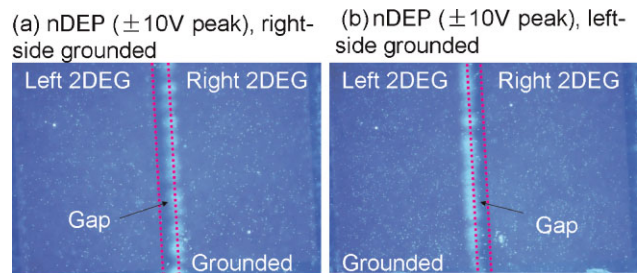


**Figure 7** (online color at: [www.pss-a.com](http://www.pss-a.com)) The microspheres once levitated moved toward the 2DEG electrode that was grounded: (a) right-side grounded; (b) left-side grounded. The dotted lines demarcate the edges of the 2DEG electrodes.

These particular 2DEG electrodes were grounded and the negatively charged microspheres appeared to have preference toward the ground electrode due to the voltage offset. This observation is further shown on a simple stripe pattern of 2DEG electrodes in Fig. 7. The microspheres were initially concentrated in the gap between the 2DEG electrodes but after being levitated, moved toward the 2DEG electrode that was held at the ground potential (Fig. 7a: right-side grounded; Fig. 7b: left-side grounded).

The model proposed in Fig. 6 requires further validation by additional experiments. For instance, one may use positively charged microspheres to test the model. In fact, we switched the polarity of surface charge of  $2 \mu\text{m}$  microspheres by coating them with positive polyelectrolyte (poly-L-lysine) molecules. We confirmed the charge polarity reversal by measuring surface zeta potential of the microspheres before and after the coating, registering a value,  $-45$  and  $+40 \text{ mV}$ , respectively. Nevertheless, for the reasons unclear at the moment, these surface-modified microspheres failed to produce a noticeable response to the excitation signals applied up to  $1 \text{ MHz}$  and  $\pm 10 \text{ V}$  peak. Given the fact that the microspheres did not appear to be immobilized on the device surface, it would be reasonable to believe that the coating might have interfered with the CM factor of the microspheres.

Lastly, one might rightfully consider electrokinetic effects, apart from DEP (e.g., electroosmosis, electrophoresis) to be responsible, at least partially, for the reported phenomenon. However, we intentionally avoided here low frequencies where such effects are believed to surface. We rule out electrophoresis due to high frequencies applied and the symmetric configuration of the 2DEG layout. We believe that we could also rule out nonlinear electrokinetic effects since the operating frequencies were extremely high for the charge clouds to have adequate time to form around polarizable microspheres and electrodes [29].

**5 Conclusions** In our previous study, patterned 2DEG electrodes in AlGaIn/GaN heterostructure have been employed to generate useful DEP forces. Here, a peculiar encounter that deviates from the earlier accounts of DEP manipulation is reported for the 2DEG electrodes under the

UV illumination. The microspheres have been repelled from the 2DEG electrodes yet remained on the surface during pDEP and then levitated upon switching to nDEP. A plausible explanation of the underlying mechanism is also given based on the UV-induced generation of electron–hole pairs and the subsequent charge redistribution in the AlGaIn/GaN heterostructure.

**Acknowledgements** This project is supported by the Hong Kong Research Grant Council under grant 611809 and the Direct Allocation Grant DAG09/10.EG09.

## References

- [1] T. B. Jones, *Electromechanics of Particles* (Press Syndicate of the University of Cambridge, New York, 1995).
- [2] P. R. C. Gascoyne and J. Vykoukal, *Electrophoresis* **23**, 1973 (2002).
- [3] H. Morgan, M. P. Hughes, and N. G. Green, *Biophys. J.* **77**, 516 (1999).
- [4] Z. Gagnon, S. Senapati, and H. C. Chang, *Electrophoresis* **31**, 666 (2010).
- [5] W. B. Betts, *Trends Food Sci. Technol.* **6**, 51 (1995).
- [6] L. J. Yang, *Talanta* **80**, 551 (2009).
- [7] C. Dalton and K. Kaler, *Sens. Actuators B* **123**, 628 (2007).
- [8] S. Y. Ng, J. Reboud, K. Y. P. Wang, K. C. Tang, L. Zhang, P. Wong, K. T. Moe, W. Shim, and Y. Chen, *Biosens. Bioelectron.* **25**, 1095 (2010).
- [9] S. K. Srivastava, J. I. Baylon-Cardiel, B. H. Lapizco-Encinas, and A. R. Minerick, *J. Chromatogr. A* **1218**, 1780 (2011).
- [10] K. H. Kang, Y. J. Kang, X. C. Xuan, and D. Q. Li, *Electrophoresis* **27**, 694 (2006).
- [11] E. B. Cummings and A. K. Singh, *Anal. Chem.* **75**, 4724 (2003).
- [12] B. H. Lapizco-Encinas, R. V. Davalos, B. A. Simmons, E. B. Cummings, and Y. J. Fintschenko, *Microbiol. Methods* **62**, 317 (2005).
- [13] J. L. Baylon-Cardiel, N. M. Jesus-Perez, A. V. Chavez-Santoscoy, and B. H. Lapizco-Encinas, *Lab Chip* **10**, 3235 (2010).
- [14] C. F. Chou, J. O. Tegenfeldt, O. Bakajin, S. S. Chan, E. C. Cox, N. Darnton, T. Duke, and R. H. Austin, *Biophys. J.* **83**, 2170 (2002).
- [15] B. G. Hawkins, A. E. Smith, Y. A. Syed, and B. J. Kirby, *Anal. Chem.* **79**, 7291 (2007).
- [16] J. J. Zhu and X. C. Xuan, *Electrophoresis* **30**, 2668 (2009).
- [17] F. S. S. Hardt, *Microfluidic Technologies for Miniaturized Analysis Systems* (Springer, New York, 2007).
- [18] P. Sabounchi, A. M. Morales, P. Ponce, L. P. Lee, B. A. Simmons, and R. V. Davalos, *Biomed. Microdevices* **10**, 661 (2008).
- [19] H. Shafiee, J. L. Caldwell, M. B. Sano, and R. V. Davalos, *Biomed. Microdevices* **11**, 997 (2009).
- [20] H. Shafiee, M. B. Sano, E. A. Henslee, J. L. Caldwell, and R. V. Davalos, *Lab Chip* **10**, 438 (2010).
- [21] J. Fu and K. J. Chen, *Phys. Status Solidi C* **8**, 2479 (2011).
- [22] O. Ambacher, J. Smart, J. R. Shealy, N. G. Weimann, K. Chu, M. Murphy, W. J. Schaff, and L. F. Eastman, *J. Appl. Phys.* **85**, 3222 (1999).
- [23] J. P. Ibbetson, P. T. Fini, K. D. Ness, S. P. DenBaars, J. S. Speck, and U. K. Mishra, *Appl. Phys. Lett.* **77**, 250 (2000).
- [24] Y. Cai, Z. Q. Cheng, W. C. W. Tang, K. M. Lau, and K. J. Chen, *IEEE Trans. Electron Devices* **53**, 2223 (2006).
- [25] R. N. Wang, Y. Cai, W. Tang, K. M. Lau, and K. J. Chen, *IEEE Electron Device Lett.* **27**, 633 (2006).
- [26] S. W. Lee, H. Li, and R. Bashir, *Appl. Phys. Lett.* **90**, 223902 (2007).
- [27] C. Li, D. Holmes, and H. Morgan, *Electrophoresis* **22**, 3893 (2001).
- [28] I. Ermolina and H. Morgan, *J. Colloid Interface Sci.* **285**, 419 (2005).
- [29] A. Castellanos, A. Ramos, A. Gonzalez, N. G. Green, and H. Morgan, *J. Phys. D: Appl. Phys.* **36**, 2584 (2003).